Mirel Ajdaroski
Department of Mechanical Engineering,
University of Michigan-Dearborn,
4901 Evergreen Road,
Dearborn, MI 48128
e-mail: majdaros@umich.edu

James A. Ashton-Miller
Department of Mechanical Engineering,
University of Michigan-Ann Arbor,
3443 GGB (George G. Brown Laboratory),
2350 Hayward Street,
Ann Arbor, MI 48109
e-mail: jaam@umich.edu

So Young Baek
Department of Mechanical Engineering,
University of Michigan-Ann Arbor,
3443 GGB (George G. Brown Laboratory),
2350 Hayward Street,
Ann Arbor, MI 48109
e-mail: soy@umich.edu

Payam Mirshams Shahshahani
Department of Mechanical Engineering,
University of Michigan-Ann Arbor,
3443 GGB (George G. Brown Laboratory),
2350 Hayward Street,
Ann Arbor, MI 48109
e-mail: mirshams@umich.edu

Amanda O. Esquivel
Department of Mechanical Engineering,
University of Michigan-Dearborn,
4901 Evergreen Road,
Dearborn, MI 48128
e-mail: aoe@umich.edu

Testing a Quaternion Conversion Method to Determine Human Three-Dimensional Tibiofemoral Angles During an In Vitro Simulated Jump Landing

Lower limb joint kinematics have been measured in laboratory settings using fixed camera-based motion capture systems; however, recently inertial measurement units (IMUs) have been developed as an alternative. The purpose of this study was to test a quaternion conversion (QC) method for calculating the three orthogonal knee angles during the high velocities associated with a jump landing using commercially available IMUs. Nine cadaveric knee specimens were instrumented with APDM Opal IMUs to measure knee kinematics in one-legged 3–4× bodyweight simulated jump landings, four of which were used in establishing the parameters (training) for the new method and five for validation (testing). We compared the angles obtained from the QC method to those obtained from a commercially available sensor and algorithm (APDM Opal) with those calculated from an active marker motion capture system. Results showed a significant difference between both IMU methods and the motion capture data in the majority of orthogonal angles ($p < 0.01$), though the differences between the QC method and Certus system in the testing set for flexion and rotation angles were smaller than the APDM Opal algorithm, indicating an improvement. Additionally, in all three directions, both the limits of agreement and root-mean-square error between the QC method and the motion capture system were smaller than between the commercial algorithm and the motion capture. [DOI: 10.1115/1.4052496]

1 Introduction

Over the last 20 years in the United States, the rate of anterior cruciate ligament (ACL) tears in young athletes has seen an annual increase of 2.3%, accounting for nearly half of all knee injuries [1,2]. Additionally, young female athletes sustain ACL injuries at a higher rate, with anatomic, hormonal, and biomechanical differences between the sexes being potential risk factors [3–6]. While anatomical and hormonal factors are not easily modifiable, identifying and modifying the biomechanical factors may be possible. ACL tears are generally divided into two categories: contact or noncontact in nature, with the latter defined as involving no direct contact with another player or equipment. These noncontact ACL injuries can be caused by a singular event (an acute failure), but recently repetitive, high stress- and strain-inducing activities have also been shown to lead to noncontact ACL injuries (a material fatigue failure) [7].

The majority (75%) of reported ACL injuries are noncontact injuries [8,9]. In one injury scenario, the knee is externally rotated with a slight flexion and a slight valgus angle at the time of injury [3,10]. It has been theorized that once these conditions are met and the ground reaction force is applied across the knee, a powerful quadriceps contraction can cause sufficient anterior displacement of the tibia relative to the femur that increases ACL strain above its injury threshold [3,10]. So, the magnitudes of the ground reaction and quadriceps forces, along with the three-dimensional (3D) tibiofemoral angles, are important factors [3,11].

Traditionally, lower limb joint kinematics have been observed in laboratory settings using fixed camera-based motion capture systems; however, in recent years, wearable sensors worn on selected body segments have been developed as an alternative and employed in various applications such as gait analysis and rehabilitation assistance [12–18]. One type of wearable sensor, an inertial measurement unit (IMU), consisting of three orthogonal accelerometers, rate gyroscopes, and magnetic field sensors, provides direct measures of body segment linear acceleration, angular velocity, and magnetic field strength. Additionally, 3D joint angle kinematics can be determined though methods similar to those of camera-based systems and have been evaluated and confirmed in previous studies [16,19]. IMUs provide the opportunity to monitor joint kinematics in real-world settings.

A commercially available IMU, APDM Opal (APDM Wearable Technologies, Portland, OR), uses a proprietary sensor fusion algorithm, whereby the orientation of the device can be tracked in inertial space. The algorithm uses knowledge of its dynamics to propagate the orientation changes based on gyroscope data and fuses the estimate with orientation estimates determined through its accelerometer and magnetometer information, thereby

Manuscript received March 27, 2021; final manuscript received September 18, 2021; published online November 9, 2021. Assoc. Editor: Bruce MacWilliams.

Table 1 Specimen demographics

Demographics of the specimens used in testing algorithm

Specimen #	Sex	Age	Side	Weight (kg)	Total testing trials	Trials analyzed
1	F	20	L	86.6	100	80
2	M	32	R	68.0	100	96
3	M	32	R	88.4	100	98
4	M	25	R	86.2	100	96
5	M	33	R	49.9	100	96

Demographics of specimens used for determining QC method parameters

Specimen #	Sex	Age	Side	Weight (kg)	Total testing trials	Trials analyzed
6	M	39	L	54.4	100	96
7	F	30	R	82.1	53	50
8	M	29	R	74.8	100	96
9	F	28	R	63.5	100	98

Total number of testing trials denotes how many trials the specimen was able to undergo before failure occurred, while trials analyzed consist of all trials in where refreezing of the tendon clamps was not performed nor any other noted deviations from the normal testing procedures occurred.

determining the orientation of the sensors in space. However, because this algorithm was developed for gait analysis, we hypothesized that it may not necessarily be accurate when used in more dynamic activities such as sports when larger changes in joint angles, velocity, and acceleration occur. So, the purpose of this study was to develop an algorithm to calculate the 3D tibiofemoral angles and compare those calculated angles as well as those obtained through the APDM fusion algorithm, to those from a standard motion capture system at a specific moment in time. Our goal was to determine if the new algorithm demonstrated improved accuracy and reliability in the ability to measure angles during more dynamic activities. Improvements in the ability to accurately and reliably measure tibiofemoral angles during dynamic actions could be vital in identifying and tracking potentially injurious loading cycles during on field activities and help prevent catastrophic failures such as ACL ruptures.

2 Materials and Methods

2.1 Subjects and Instrumentation. Nine cadaveric knee specimens were used for this study (Table 1). Each specimen was dissected leaving the ligamentous capsular intact as well as the muscle tendons of the quadriceps, hamstrings, and gastrocnemius. After dissection, the distal tibia/fibula and proximal femur were cut to a standard length of 20 cm from the center of the knee joint, then potted in polymethylmethacrylate cylinders. Once prepared, each specimen was rigidly fixed in a custom-built testing rig that was designed to simulate a one-legged jump landing of 3–4× bodyweight (Fig. 1). This testing rig, which includes simulated trans-knee muscle forces, has been validated in previous studies [20,21].

A Certus optoelectronic tracking system (OPTOTRAK CERTUS; Northern Digital Inc., Waterloo, ON, Canada) was used to track the changes in 3D tibiofemoral angles during the jump landing. A total of 20 Certus markers were used. Two sets of three "real" markers (physical markers affixed to a rigid body) were placed on the tibial and femoral load cells. An additional 14 "imaginary" markers were used that represented the anatomic landmarks of the knee being tested. This allowed for the capture of tibiofemoral kinematics such as 3D translation and rotation of the tibia with respect to the femur. The use of a 3D digitizing wand allowed for the defining and tracking of each imaginary marker. The sampling rate for the Certus system was set to 2 kHz. An APDM Opal sensor was rigidly attached to the medial aspect of the midtibia and another to the lateral aspect of the midfemur using Co-flex bands and elastic ties (Fig. 1). The sampling rate for the APDM Opal sensors was 256 Hz, but was expanded through linear interpolation to have a sampling rate of 2048 Hz in order to compare with the Certus system.

2.2 Testing Procedure. Before testing began, the IMU sensors were calibrated through the predefined calibration conditions used by the MOVEO MOBILITY software developed by APDM. This initialization process was used by the software to establish initial conditions and minimize the influence that drift may have on data validity. Once initialized, the sensors continuously recorded data. After initialization, the quadriceps, hamstring, and gastrocnemius muscles were pretensioned to 180 N, 70 N, and 70 N, respectively, the initial knee angle adjusted to 15 deg, and clamped securely in place with mechanical grips cooled by liquid nitrogen. This last step had to be repeated periodically throughout the testing, so

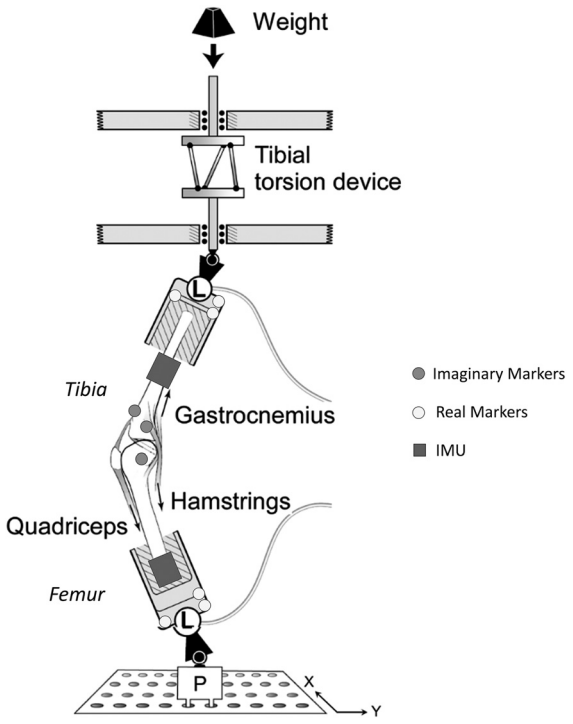

Fig. 1 Schematic of test setup (reproduced with permission)

knee angle and muscle tensions were recorded prior to each test and adjusted back to the above values, if necessary.

Drop height and weight were adjusted to match the target tibial ground reaction impact force of 4× bodyweight (for larger specimens, this was reduced to 3× bodyweight so as not exceed test rig capacity). Once established, impacts were initiated by releasing a large weight to impact the distal end of the tibial load cell (Fig. 1) guided via two parallel linear bearings. At least five preconditioning trials were conducted before the activation of the tibial torsional device to allow for any adjustments, and for potential uncrimping of collagen fibers. The tibial torsional device allowed for some of the impact force to be converted to internal tibial torque, as can happen in a live subject when the ground reaction causes internal tibial rotation at the knee [20,21]. After the activation of the tibial torsional device, each specimen was subjected to up to 100 trials or until knee failure occurred, clinically defined as anterior tibial displacement in excess of 3 mm. Peak impact force was typically reached around 70 ms, so each trial consisted of 200 ms of data.

2.3 Data Analysis. In this study, we compared changes in tibiofemoral flexion, abduction, and internal rotation angles at peak impact with the three measurement modalities: (1) the Certus measurements which we considered "gold standard" for this study, and APDM wearable sensors—(2) using their proprietary algorithm, and (3) our proposed algorithm. It was assumed that maximum vertical linear acceleration as measured by the APDM Opal sensors occurred at the same time as the maximum vertical force as measured by the Certus system. This assumption was made based on previous studies that showed strong correlation between ground reaction force and linear acceleration [22].

2.3.1 Calculating the Euler Angles. A nine-axis indirect Kalman filter using the quaternion conversions of the IMU accelerometer, gyroscope, and magnetometer data was used in this study. This process is detailed at greater length in the paper by Stanley et al. [23]. Briefly, data were filtered using a fourth-order, zero-lag, low pass Butterworth filter. Optimum cutoff frequency for the Butterworth low-pass digital filter was obtained by applying Winters' method to the sum squared difference between the unfiltered data and filtered data at a given frequency lying within the range of $1 \leq x < \frac{\text{sampling rate}}{2}$, divided by the sum squared difference between unfiltered data and the unfiltered mean; this process is outlined further by Yu et al. [24]. Average optimal cutoff frequencies were determined as: 12 Hz for the accelerometer ($X = 19$ Hz; $Y = 11$ Hz; $Z = 7$ Hz); 20 Hz for the gyroscope ($X = 10$ Hz; $Y = 42$ Hz; $Z = 9$ Hz); and 8 Hz for the magnetometer ($X = 5$ Hz; $Y = 10$ Hz; $Z = 10$ Hz). After filtering, a predicted orientation, v_i, for the current frame from the angular change of the previous frame, v_{i-1}, was obtained and subsequently converted to a quaternion such that

$$v_i = R_i^f H \otimes v_{i-1} \tag{1}$$

where $R_i^f H$ is a rotation matrix from the inertial frame to the body frame using quaternion elements. Initially, the predicted orientation was estimated to be north-east-down. Additionally, the previous orientation estimate q^- was updated by rotating it by v_i such that

$$q^- = q^+\left(\prod_{n=1}^{i} v_n\right) \tag{2}$$

Using the quaternion conversions, estimations of gravitational and magnetic field measurements were obtained using the linear acceleration and angular velocity. These estimates were used to correct the gravitational and magnetic field data obtained by the previous orientation and magnetometer. These corrected estimates became the innovation, y_k, for the indirect Kalman filter. As mentioned by Stanley et al., the indirect Kalman filter attempts to track errors rather than orientation as the data are updated through a recursive process [23]. Additionally, because the process is recursive, the a priori estimates of the error process and the state transition models are always zero [23]. Therefore, the Kalman equations utilized in this study were reduced to

$$P_k^- = Q_k \tag{3}$$

$$S_k = R_k - H_k P_k^- H_k^T \tag{4}$$

$$K_k = P_k^- H_k^T (S_k)^{-1} \tag{5}$$

$$x_k^+ = K_k y_k \tag{6}$$

$$P_k^+ = P_k^- - K_k H_k P_k^- \tag{7}$$

where S_k is defined as the innovation covariance, R_k is the covariance of the observation model noise, H_k is the observation model, P_k^- is the predicted estimate covariance, K_k is the Kalman Gain, P_k^+ is the updated estimate covariance, and x_k^+ is the a posteriori state estimate. The a posteriori state estimate's orientation was corrected by previous estimation such that

$$q_k^+ = (q_k^-)(x_k^+) \tag{8}$$

Because the orientation was still in quaternion format, subtraction of the data from two adjacent segments is mathematically valid. Therefore, the data attributed to the tibial IMU sensor were subtracted from the femoral IMU sensor. The resulting values were then converted into Euler angles through:

$$\phi = a\tan 2\Big(2(q_1 q_2 + q_2 q_3), 1 - 2\big(q_2^2 + q_3^2\big)\Big) \tag{9}$$

$$\theta = a\sin\big(2(q_1 q_3 - q_4 q_2)\big) \tag{10}$$

$$\psi = a\tan 2\Big(2(q_1 q_4 + q_2 q_3), 1 - 2\big(q_3^2 + q_3^2\big)\Big) \tag{11}$$

where ϕ is the internal/external rotation, θ is the valgus/varus angle, and ψ is the flexion/extension angle.

2.3.2 Establishing the Parameters. The covariance of the observation model noise, R_k, as well as the predicted estimate covariance, P_k^-, consisted of several parameters unique to a sensor. These unique parameters included accelerometer noise (variance of accelerometer signal noise), linear acceleration noise (variance of linear acceleration noise; akin to gyroscope drift noise), gyroscope drift noise (variance of gyroscope offset drift), gyroscope noise (variance of gyroscope single noise), magnetic disturbance noise (variance of the magnetic disturbance noise), magnetometer noise (variance in the magnetometer signal noise), linear acceleration decay factor (decay factor for the linear acceleration), and magnetic disturbance decay factor (decay factor for the magnetic disturbance) [23]. APDM Opal documentation provided the values associated with accelerometer noise, gyroscope noise, and magnetometer noise. The parameters of gyroscope drift noise, linear acceleration noise, and magnetic disturbance noise were not detailed by the documentation, and instead default values based on the FRDM-FXS-Multifamily of sensor boards (as used by the Freescale Toolbox of MATLAB) were used. The use of these default values was implemented due to the potential value ranges being theoretically infinite such that a process of trial and error would not be possible. Linear acceleration decay factor (LADF) and magnetic disturbance decay factor (MDDF) were unknown parameters that could be adjusted as their theoretical values ranged from 0 to 1. Therefore, of the nine specimens in this study, four were selected to establish the values of these parameters (training set) (Table 1). A trial-and-error approach was taken where adjustments to the LADF and/or MDDF were performed to

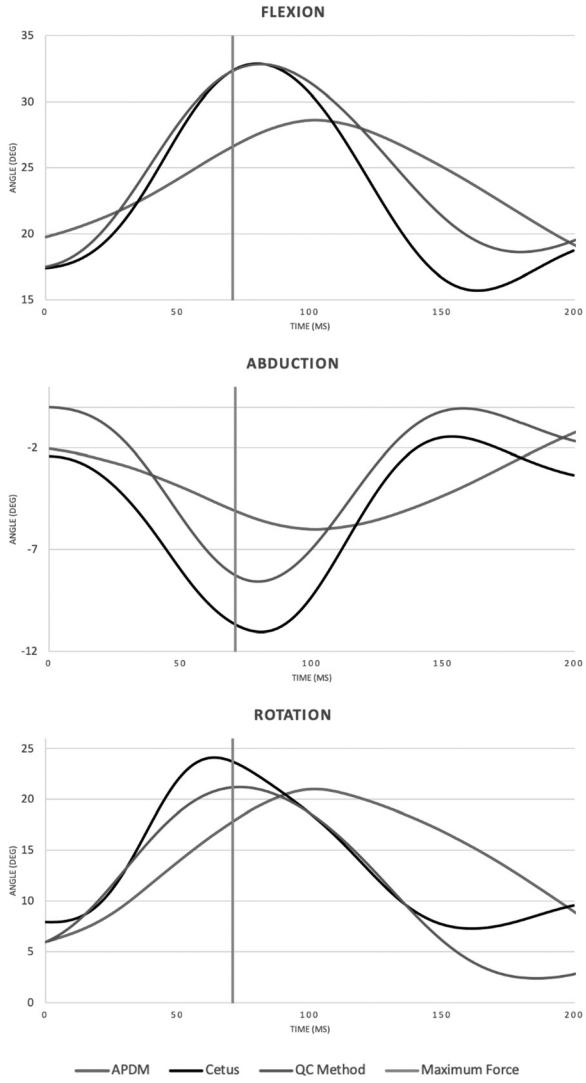

Fig. 2 Average time history of each orthogonal knee angle as measured by APDM algorithm (top curve), Certus (bottom most curve) and QC method (middle curve) for a single knee specimen for (*a*) flexion, (*b*) abduction, and (*c*) rotation. The vertical line indicates the time of the peak impact force. Note: Consistently, the APDM algorithm (bottom most curve) exhibited a phase lag relative to the Certus and QC method.

minimize the difference in maximum angle between the quaternion conversion (QC) method and the Certus system. These adjustments were performed on each of the three orthogonal angles resulting in three unique LADF and three unique MDDF values per specimen. An average for both LADF and MDDF was determined and used when calculating the angles of the remaining five specimens (testing set). A trial-and-error approach was used as it requires no assumed knowledge of the system and allows for the determination of some valid working solution. MATLAB scripts were used to calculate specimen angles using the QC method for both the training set and testing set (MATLAB_R2019b; MathWorks, Natick, MA).

2.4 Statistical Analysis. Since the intermittent freezing of the patellar ligament clamp led to significant changes in linear acceleration and angular velocity and had the potential to affect the mechanical properties of the specimen immediately postfreezing, these trials were omitted from any analysis. A repeated measures analysis of variance with a pairwise comparison was performed on both training and testing specimen sets to determine whether there was a difference between the QC method and the Certus data, the QC method and the APDM algorithm, and the APDM algorithm and the Certus data (IBM SPSS Statistics v 24.0). A Bonferroni correction was used to correct for multiple comparisons. Differences were considered significant if $p < 0.05$. Bland–Altman limits of agreement (LoA) were constructed for the testing specimen set in order to examine each method's reliability; lower LoA values indicated a better degree of reliability [25]. Linear mixed effect models for both sets were constructed where the angle as measured by Certus was a linear function of the IMU angles (the QC method or the APDM algorithm) with a random intercept per specimen. The root-mean-square of the residuals of the linear mixed effect model was used as the root mean squared error (RMSE) between Certus and one of the IMU angle methods.

3 Results

The angles of interest were those that occurred at maximum vertical tibial force (Certus system) or at maximum vertical tibial linear acceleration (APDM Opal and QC method) during the simulated jump "landing." Figure 2 illustrates the representative signals measured by the three systems as well as the timestamp of the angle of interest. The APDM Opal algorithm exhibited a phase lag, whereby the peak angle appeared at a later time than the peak angle of either the Certus system or the QC method.

3.1 Training Set. There was a significant difference in all three angles between the Certus and APDM Opal algorithm. The training set showed a mean difference in flexion/extension between the Certus system and APDM Opal algorithm of 0.9 deg (95% CI: 0.6 deg to 1.2 deg) (Table 2). For abduction/adduction, a mean difference of −1.1 deg (95% CI: −1.1 deg to −0.5 deg) between the Certus system and APDM Opal algorithm was observed, while the mean difference between the Certus system and the QC method was 0.2 deg (95% CI: 0.1 deg to 0.3 deg) (Table 2). The mean difference in rotation between the Certus system and APDM Opal algorithm was 2.7 deg (95% CI: 2.1 deg to 3.3 deg) (Table 2). In each case, both the LoA and RMSE associated with QC method versus Certus were observed to be smaller, indicating an increase in accuracy and reliability when using the QC method (Table 3).

3.2 Testing Set. There was a statistically significant difference between the Certus measurements and both the QC Method and APDM Opal algorithm for all three angles. There was a mean difference in flexion/extension of 2.5 deg (95% CI: 2.0 deg to 3.1 deg) between the Certus system and APDM Opal algorithm while the mean difference between the Certus system and the QC method was −0.7 deg (95% CI: −1.1 deg to 0.4 deg) (Table 2). For abduction/adduction, the mean difference between the Certus system and APDM Opal algorithm was −4.1 deg (95% CI: −4.3 deg to −3.9 deg) while the mean difference between the Certus system and the QC method was −1.2 deg (95% CI: −1.4 deg to −1.0 deg) (Table 2). For rotation, the mean difference between the Certus system and APDM Opal algorithm was 6.7 deg (95% CI: 5.8 deg to 7.6 deg) while the mean difference between the Certus and the QC method was observed to be 1.0 deg (95% CI: 0.6 deg to 1.4 deg) (Table 2).

The Bland–Altman plot for flexion/extension of APDM algorithm versus Certus cases showed a downward trend, indicating that the APDM algorithm method tended to overestimate the angle at lower angles and underestimate it at higher ones while no such trend was observed in QC method versus Certus (Fig. 3(*a*)). The majority of trials for APDM algorithm versus Certus fell below the zero-difference line, indicating a tendency for underestimation while QC Method versus Certus demonstrated a tendency for overestimation. For abduction/adduction, both APDM algorithm versus Certus and QC method versus Certus showed a downward trend; however, the trend associated with QC method

Table 2 Values of the pairwise comparison analysis performed for (a) flexion, (b) abduction, (c) rotation in degrees

Repeated measures analysis of variance with pairwise comparison					
		Training set		Testing set	
	Comparison	Mean diff. (SD)	95% CI[a]	Mean diff. (SD)	95% CI[a]
Flexion	Certus versus APDM algorithm	0.9 deg (2.8 deg)*	(0.6 deg, 1.2 deg)	2.5 deg (0.2 deg)*	(1.9 deg, 3.1 deg)
	Certus versus QC Method	−0.1 deg (0.9 deg)	(−0.2 deg,0.0 deg)	−0.7 deg (0.1 deg)*	(−1.1 deg, −0.4 deg)
	QC Method versus APDM algorithm	−0.8 deg (2.8 deg)*	(−1.1 deg, −0.5 deg)	3.2 deg (0.3 deg)*	(2.6 deg, 3.8 deg)
Abduction	Certus versus APDM algorithm	−1.1 deg (2.8 deg)*	(−1.4 deg, −0.8 deg)	−4.1 deg (0.1 deg)*	(−4.3 deg, −3.9 deg)
	Certus versus QC Method	0.2 deg (0.7 deg)*	(0.1 deg, 0.3 deg)	−1.2 deg (0.1 deg)*	(−1.4 deg, −1.0 deg)
	QC Method versus APDM algorithm	0.9 deg (2.7 deg)*	(0.7 deg, 1.2 deg)	−2.9 deg (0.1 deg)*	(−3.2 deg, −2.6 deg)
Rotation	Certus versus APDM algorithm	2.7 deg (5.9 deg)*	(2.1 deg, 3.3 deg)	6.7 deg (0.4 deg)*	(5.8 deg, 7.6 deg)
	Certus versus QC Method	0.1 deg (1.5 deg)	(−0.1 deg, 0.2 deg)	1.0 deg (0.2 deg)*	(0.6 deg, 1.4 deg)
	APDM algorithm versus QC Method	−2.8 deg (5.9 deg)*	(−3.4 deg, −2.2 deg)	5.7 deg (0.4 deg)*	(4.8 deg, 6.5 deg)

Mean (SD) and 95% confidence interval (CI) are based on the difference in angle measurement between compared systems for specimens in the training algorithm set (left) and for those in the testing algorithm set (right).
[a]Adjustment for multiple comparison: Bonferroni.
*Statistically significant $p < 0.05$.

Table 3 Comparison of the calculated knee angles between IMU based methods (APDM Opal or QC Method) and the Certus motion capture system for specimens in the training algorithm set (left) and for those in the testing algorithm set (right)

Comparison of IMU methods to Certus values					
		Training set		Testing set	
	Comparison	RMSE	LoA	RMSE	LoA
Flexion	Certus versus APDM algorithm	1.0 deg	(−6.3, 4.6)	3.1 deg	(−12.1 deg, 7.0 deg)
	Certus versus QC Method	0.7 deg	(−1.9, 1.8)	2.6 deg	(−4.5 deg, 5.8 deg)
Abduction	Certus versus APDM algorithm	2.0 deg	(−4.4, 6.7)	1.1 deg	(0.2 deg, 8.0)
	Certus versus QC Method	0.7 deg	(−1.3, 1.7)	0.8 deg	(−2.1 deg, 4.4 deg)
Rotation	Certus versus APDM algorithm	3.4 deg	(14.2, 8.8)	6.0 deg	(−22.5 deg, 9.2 deg)
	Certus versus QC Method	1.5 deg	(−2.9, 3.1)	2.4 deg	(−8.6 deg, 6.6 deg)

versus Certus was less pronounced (Fig. 3(*b*)). Both APDM versus Certus and QC Method versus Certus exhibited a majority of trials above the zero-difference line indicating a tendency for underestimation of the Certus absolute angle, though APDM algorithm versus Certus exhibited a greater propensity (3.4% versus 23.0%). In the Bland–Altman plot for rotation, both APDM algorithm versus Certus and QC method versus Certus showed similar downward trends with both exhibiting the majority of their trials falling below the zero-difference line indicating a tendency of underestimation in both methods (Fig. 3(*c*)). Though again, APDM algorithm versus Certus exhibited a greater propensity for underestimation (79.4% versus 63.4%). Additionally, in each case, both the LoA and RMSE associated with QC method versus Certus were observed to be smaller than the opal algorithm, indicating an increase in accuracy and reliability when using the QC method and the training set LoA and RMSE were lower than the testing set (Table 3).

4 Discussion

The purpose of this study was to determine whether the QC method could provide improved accuracy and reliability measurements of the changes in 3D knee angles during a dynamic activity consisting of a jump landing. In this study, we observed that across all cases and specimen sets, the QC method produced smaller differences than APDM algorithm when compared to the "gold-standard" Certus motion capture system. Although in that majority of cases, the difference between the QC method and Certus was statistically significant ($p < 0.01$), the mean difference for flexion (−0.7 deg) and rotation (1.0 deg) in the testing set between the two systems is clinically insignificant. For example, a review paper that examined the difference in knee flexion angles during documented ACL tears in male and female athletes reported differences in 10 deg to 21.7 deg in knee flexion between injured and uninjured athletes and a laboratory study found a correlation of increased abduction angle of 8 deg in female athletes who went on to injure their ACL [26,27]. Only the mean difference between the QC method and Certus for flexion (−0.1 deg) and rotation (0.1 deg) in the training set were observed as not being statistically significant, though this may be due to the algorithm being overly tuned for the training set. Furthermore, in every instance the RMSE values associated with the difference between the QC method and the Certus system were smaller than those for the APDM algorithm, with the largest difference occurring in the testing set for rotation (2.4 deg compared to 6.0 deg). In every case the LoA associated with the difference between the QC method and the Certus system was smaller than those of APDM Opal, indicating a smaller range in differences and better degree of reliability. A particular point of interest is the observation that the APDM Opal algorithm exhibited a phase lag compared to the Certus system, whereas the QC method did not (Fig. 2). This was also observed by Takeda et al. where a phase lag in peak flexion angle between the IMU and camera system is visible [28]. Takeda et al. attributed this phase lag in their study to the use of a moving average filter to remove noise from the raw acceleration and angular velocity data [28].

A number of studies have calculated joint angles using IMU sensors and compared the results to those from a motion capture

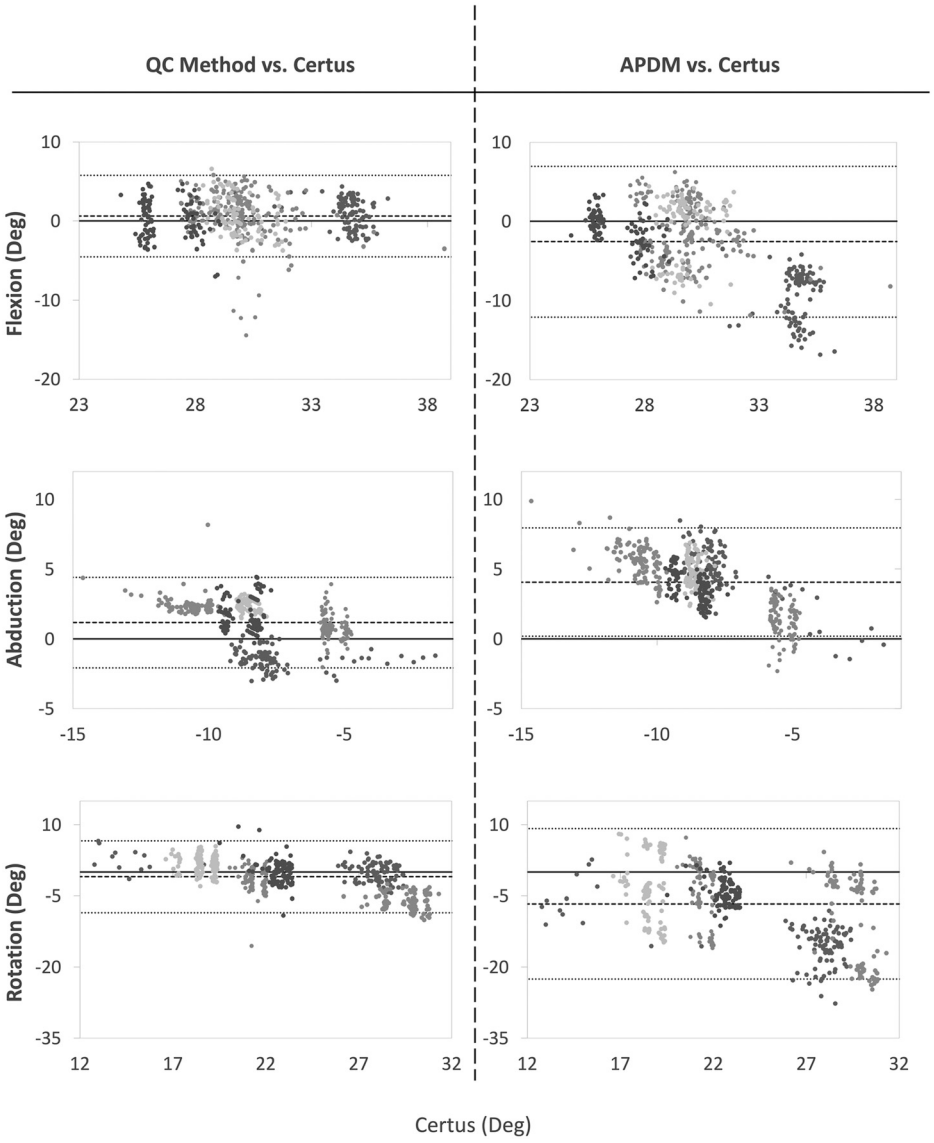

Fig. 3 Bland–Altman plot associated with the difference between the (*a*) flexion, (*b*) abduction, and (*c*) rotation of the APDM software and Certus system (left) and between the QC method and Certus (right) grouped in terms of specimen. The *y*-axis shows the difference in measured angle between the systems (either APDM-Certus or QC-Certus) while the *x*-axis shows the value of Certus.

system [28–31]. However, most focus has been on examining differences in knee flexion, the knee angle that exhibits the largest change. While determining an IMU's ability to measure flexion angles is important when observing knee injuries, a number of studies have noted the relationships between knee injuries (particularly ACL stress/strain) and valgus and rotational angles, rather than flexion angle [6,32–37]. So, for the purposes of improving knee injury prevention, it is important to be able to accurately measure all three tibiofemoral angles, not just flexion. Determining Euler angles from only linear acceleration and angular velocity is common practice because this process does have the ability to smoothly measure rotation in 3D space. However, because it can only yield orientation to some random horizontal global frame of reference, it lacks a sense of magnetic north and thus cannot accurately measure angles perpendicular to that horizontal global frame [23]. Furthermore, in many of these studies, direct conversion of angular velocities into Euler angles through the implementation of a rotation matrix was performed [28,29]. This approach poses several problems. First, rotation matrices do not commute and the order with which they are applied is important. Additionally, there is a possibility that during rotation, alignment of two of the axes may occur resulting in gimbal lock and loss of data. And finally, there is a potential distortion of the data that can occur. It should also be noted that Euler angles are not vectors. This poses the issue that, mathematically, subtraction of the Euler angles of adjacent segments to determine joint angles is not justifiable.

Studies such as those by Watanabe et al. and Tong et al. calculated knee flexion joint angles but did not convert these to Euler angles [30,31]. This poses the problem that angles obtained by either study do not describe the orientation of the joint with respect to a fixed coordinate system and thus may not represent the knee's true 3D angular orientation. In the study conducted by Tong et al., the difference between adjacent segment inclinations was determined which, when compared to their camera system, resulted in a RMSE value of 6.4 deg. This is larger than that observed within our study for either the APDM Opal (3.1 deg) or our QC Method (2.6 deg) [31]. Watanabe et al. performed a similar process to that of Tong et al. in that they used the difference in integrated angular velocity between two adjacent segments;

however, they also made use of a Butterworth low-pass filter as well as a Kalman filter, as we used in our QC Method [30]. Watanabe et al. observed a RMSE between 3 deg and 4 deg, smaller than that reported by Tong et al. and comparable to that of the APDM Opal (3.1 deg); however, the RMSE associated with our QC Method was observed to be smaller (2.6 deg). Both of these studies examined gait, which has lower velocities and accelerations than the present jump landing activity. Slower movements, such as in gait, may not have the same levels of movement artifact as those that are more dynamic such as those in this study. Additionally, Tong et al. used a limited sample size ($N = 3$), which is unlikely to suffice to establish a reliable methodology [31]. While the sample size used by Watanabe et al. was comparable to our study ($N = 6$), they had significantly fewer total trials ($N = 18$ compared to $N = 466$), which may not capture the intertrial variations and trends [30]. In addition, these studies calculated knee flexion angle only.

Takeda et al. used angular velocity of an IMU to estimate the translational acceleration; this translational acceleration was subtracted from the IMU linear acceleration to obtain gravitational acceleration, which was then used to determine flexional orientation of the joint [28]. Unlike the studies of either Watanabe et al. or Tong et al., Takeda et al. applied rotational matrices to obtain Euler angles [28]. The process resulted in an observed RMSE between their method and camera system of 6.8 deg, comparable to that observed by Tong et al. and larger than that observed within our study for either the APDM Opal (3.1 deg) or our method (2.6 deg) [28]. The lag observed by Takeda et al. between their method and camera system is similar to the lag observed in our study between APDM Opal and Certus system: their method's peak flexion angle fell between 10% and 15% after the peak flexion angle of the camera system, and in our study the average APDM Opal peak flexion angle was 40 ms (~20%) after the peak flexion angle of the camera system [28].

One previous study used APDM Opal sensors and compared the results to a camera system, but unlike many other studies made use of both highly dynamic activities (jumps) as well as live subjects [38]. Additionally, all three angles of the knee were measured and compared. The APDM Opal sensors performed well under certain conditions, primarily those of smaller angular displacement and in the ability to measure abduction/adduction and internal/external rotation [38]. This was not what was observed in our study which found abduction/adduction and internal/external rotation of either method exhibiting larger RMSE values. In nearly every case, RMSE values observed in this study were smaller than those previously reported [38]. The only exception was in the comparison of internal/external rotation for APDM Opal versus Certus, which had the largest RMSE values among all comparisons (RMSE: 6.7 deg compared to 3.9 deg observed by Ajdaroski et al.) [38]. While artifact due to skin/muscle laxity of live subjects may have contributed to why the RMSE values observed were larger, in the case of internal/external rotation of APDM Opal versus Certus it may be drift and error accumulation due to the longer testing durations in this study that could account for its larger RMSE value. The QC method has the potential for measuring more accurate and more reliable angles than the method employed by APDM Opal algorithm, although application of the QC method on live subjects is still needed to confirm this.

4.1 Limitations. This study examined a new algorithm for calculating knee angles in a "best case scenario" without the ever-present soft tissue motion that affects the coupling of the sensor to the bone in vivo. That means that the present measurements of knee angle changes were conducted under the best possible conditions and future studies should examine how soft tissue motion can affect accuracy. Additional pre-/postfiltering may be necessary when using the QC method in live subjects. Additional variation may also be expected in live subjects because each individual will have more varied landing kinematics than the present instrumented apparatus provided. It is also true that limited ranges in flexion, abduction, and rotation angles were observed in this study. In order to understand the possible error that could occur in the full range of motion of the knee, testing with both smaller and larger knee angle changes will be required. Furthermore, maneuvers other than jump landings have been observed to lead to non-contact ACL injuries and as such, it may be possible that the QC method developed in this study is overly tuned for a jump landing scenario [11–13]. The trial-and-error approach used in determination of LADF and MDDF values may be a source of potential error. A more robust method such as a nonlinear programming with specific constraint conditions could have been used, although it should be noted that this can be expensive to perform and given the very small differences between the QC method and Certus, the added precision in value may not be needed. The limited number of specimens ($n = 4$) used to establish the parameters for the QC method is also a potential limitation. The lower sampling rate of the IMU may also be a limitation as this may have led to missed information and/or aliasing when compared to higher sampling rates. Finally, the presence of iron in the frame of the present apparatus might have affected the accuracy of the IMU magnetometer readings, a situation that would not exist on a large outdoor field.

Conclusions

The QC method was able to more accurately estimate knee angles during a simulated one-legged landing than the APDM Opal algorithm across all three tibiofemoral angles. The improvements in accuracy provided by the QC method demonstrates that it may be feasible to use IMUs to identify and track knee angle measurements that may be associated with ACL injury given the reported association between ACL stress/strain and knee valgus and internal rotation angles and moments. Further testing of the QC method is needed in live subjects and in a variety of scenarios.

Acknowledgment

The authors wish to thank Dr. Melanie Beaulieu for her assistance with data collection.

Funding Data

- National Science Foundation (Grant No. 2003434; Funder ID: 10.13039/100000001).
- National Institutes of Health (Award No. AR054821; Funder ID: 10.13039/100000002).

References

[1] Musahl, V., and Karlsson, J., 2019, "Anterior Cruciate Ligament Tear," N. Engl. J. Med., **380**(24), pp. 2341–2348.
[2] Beck, N. A., Lawrence, J. T. R., Nordin, J. D., DeFor, T. A., and Tompkins, M., 2017, "ACL Tears in School-Aged Children and Adolescents Over 20 Years," Pediatrics, **139**(3), p. e20161877.
[3] Griffin, L. Y., Agel, J., Albohm, M. J., Arendt, E. A., Dick, R. W., Garrett, W. E., Garrick, J. G., et alet al., 2000, "Noncontact Anterior Cruciate Ligament Injuries: Risk Factors and Prevention Strategies," J. Am. Acad. Orthop. Surg., **8**(3), pp. 141–150.
[4] Wild, C. Y., Steele, J. R., and Munro, B. J., 2012, "Why Do Girls Sustain More Anterior Cruciate Ligament Injuries Than Boys?: A Review of the Changes in Estrogen and Musculoskeletal Structure and Function During Puberty," Sports Med., **42**(9), pp. 733–749.
[5] Yin, L., Sun, D., Mei, Q. C., Gu, Y. D., Baker, J. S., and Feng, N., 2015, "The Kinematics and Kinetics Analysis of the Lower Extremity in the Landing Phase of a Stop-Jump Task," Open Biomed. Eng. J., **9**(1), pp. 103–107.
[6] Yu, B., and Garrett, W. E., 2007, "Mechanisms of Non-Contact ACL Injuries," Br. J. Sports Med., **41**(Suppl 1), pp. i47–i51.
[7] Wojtys, E. M., Beaulieu, M. L., and Ashton-Miller, J. A., 2016, "New Perspectives on ACL Injury: On the Role of Repetitive Sub-Maximal Knee Loading in Causing ACL Fatigue Failure," J. Orthop. Res., **34**(12), pp. 2059–2068.
[8] Boden, B. P., Sheehan, F. T., Torg, J. S., and Hewett, T. E., 2010, "Noncontact Anterior Cruciate Ligament Injuries: Mechanisms and Risk Factors," J. Am. Acad. Orthop. Surg., **18**(9), pp. 520–527.

[9] Launay, F., 2015, "Sports-Related Overuse Injuries in Children," Orthop. Traumatol. Surg. Res., **101**(1), pp. S139–S147.
[10] Olsen, O. E., Myklebust, G., Engebretsen, L., and Bahr, R., 2004, "Injury Mechanisms for Anterior Cruciate Ligament Injuries in Team Handball: A Systematic Video Analysis," Am. J. Sports Med., **32**(4), pp. 1002–1012.
[11] Renstrom, P., Ljungqvist, A., Arendt, E., Beynnon, B., Fukubayashi, T., Garrett, W., Georgoulis, T., et alet al., 2008, "Non-Contact ACL Injuries in Female Athletes: An International Olympic Committee Current Concepts Statement," Br. J. Sports Med., **42**(6), pp. 394–412.
[12] Anderson, C. J., Ziegler, C. G., Wijdicks, C. A., Engebretsen, L., and LaPrade, R. F., 2012, "Arthroscopically Pertinent Anatomy of the Anterolateral and Posteromedial Bundles of the Posterior Cruciate Ligament," J. Bone Jt. Surg. Am., **94**(21), pp. 1936–1945.
[13] Arif, M., and Kattan, A., 2015, "Physical Activities Monitoring Using Wearable Acceleration Sensors Attached to the Body," PLoS One, **10**(7), p. e0130851.
[14] Cutti, A. G., Ferrari, A., Garofalo, P., Raggi, M., Cappello, A., and Ferrari, A., 2010, "'Outwalk': A Protocol for Clinical Gait Analysis Based on Inertial and Magnetic Sensors," Med. Biol. Eng. Comput., **48**(1), pp. 17–25.
[15] Favre, J., Crevoisier, X., Jolles, B. M., and Aminian, K., 2010, "Evaluation of a Mixed Approach Combining Stationary and Wearable Systems to Monitor Gait Over Long Distance," J. Biomech., **43**(11), pp. 2196–2202.
[16] Ferrari, A., Cutti, A. G., Garofalo, P., Raggi, M., Heijboer, M., Cappello, A., and Davalli, A., 2010, "First In Vivo Assessment of "Outwalk": A Novel Protocol for Clinical Gait Analysis Based on Inertial and Magnetic Sensors," Med. Biol. Eng. Comput., **48**(1), pp. 1–15.
[17] Lin, J. F., and Kulić, D., 2012, "Human Pose Recovery Using Wireless Inertial Measurement Units," Physiol. Meas., **33**(12), pp. 2099–2115.
[18] Picerno, P., Cereatti, A., and Cappozzo, A., 2008, "Joint Kinematics Estimate Using Wearable Inertial and Magnetic Sensing Modules," Gait Posture, **28**(4), pp. 588–595.
[19] Favre, J., Aissaoui, R., Jolles, B. M., de Guise, J. A., and Aminian, K., 2009, "Functional Calibration Procedure for 3D Knee Joint Angle Description Using Inertial Sensors," J. Biomech., **42**(14), pp. 2330–2335.
[20] Lipps, D. B., Wojtys, E. M., and Ashton-Miller, J. A., 2013, "Anterior Cruciate Ligament Fatigue Failures in Knees Subjected to Repeated Simulated Pivot Landings," Am. J. Sports Med., **41**(5), pp. 1058–1066.
[21] Lipps, D. B., Oh, Y. K., Ashton-Miller, J. A., and Wojtys, E. M., 2014, "Effect of Increased Quadriceps Tensile Stiffness on Peak Anterior Cruciate Ligament Strain During a Simulated Pivot Landing," J. Orthop. Res., **32**(3), pp. 423–430.
[22] Elvin, N. G., Elvin, A. A., and Arnoczky, S. P., 2007, "Correlation Between Ground Reaction Force and Tibial Acceleration in Vertical Jumping," J. Appl. Biomech., **23**(3), pp. 180–189.
[23] Pedley, M., Stanley, M., and Baranski, Z., 2014, "Freescale Sensor Fusion Kalman Filter," Freescale Semiconductor, accessed Oct. 4, 2021, https://github.com/memsindustrygroup/Open-Source-Sensor-Fusion/tree/master/docs
[24] Yu, B., Gabriel, D., Noble, L., and An, K.-N., 1999, "Estimate of the Optimum Cutoff Frequency for the Butterworth Low-Pass Digital Filter," J. Appl. Biomech., **15**(3), pp. 318–329.
[25] Bland, J. M., and Altman, D. G., 1986, "Statistical Methods for Assessing Agreement Between Two Methods of Clinical Measurement," Lancet, **1**(8476), pp. 307–310.
[26] Larwa, J., Stoy, C., Chafetz, R. S., Boniello, M., and Franklin, C., 2021, "Stiff Landings, Core Stability, and Dynamic Knee Valgus: A Systematic Review on Documented Anterior Cruciate Ligament Ruptures in Male and Female Athletes," Int. J. Environ. Res. Public Health, **18**(7), pp. 3826–3839.
[27] Hewett, T. E., Myer, G. D., Ford, K. R., Heidt, R. S., Colosimo, A. J., McLean, S. G., van den Bogert, A. J., Paterno, M. V., and Succop, P., 2005, "Biomechanical Measures of Neuromuscular Control and Valgus Loading of the Knee Predict Anterior Cruciate Ligament Injury Risk in Female Athletes: A Prospective Study," Am. J. Sports Med., **33**(4), pp. 492–501.
[28] Takeda, R., Tadano, S., Natorigawa, A., Todoh, M., and Yoshinari, S., 2009, "Gait Posture Estimation Using Wearable Acceleration and Gyro Sensors," J. Biomech., **42**(15), pp. 2486–2494.
[29] Barrett, J. M., Viggiani, D., Park, J., and Callaghan, J. P., 2020, "Expressing Angles Relative to Reference Postures: A Mathematical Comparison of Four Approaches," J. Biomech., **104**, p. 109733.
[30] Watanabe, T., and Saito, H., 2011, "Tests of Wireless Wearable Sensor System in Joint Angle Measurement of Lower Limbs," 2011 Annual International Conference of the IEEE Engineering in Medicine and Biology Society, Boston, MA, Aug. 30–Sept. 3, pp. 5469–5472.
[31] Tong, K., and Granat, M. H., 1999, "A Practical Gait Analysis System Using Gyroscopes," Med. Eng. Phys., **21**(2), pp. 87–94.
[32] Markolf, K. L., Burchfield, D. M., Shapiro, M. M., Shepard, M. F., Finerman, G. A., and Slauterbeck, J. L., 1995, "Combined Knee Loading States That Generate High Anterior Cruciate Ligament Forces," J. Orthop. Res., **13**(6), pp. 930–935.
[33] Hewett, T. E., Myer, G. D., and Ford, K. R., 2006, "Anterior Cruciate Ligament Injuries in Female Athletes: Part 1, Mechanisms and Risk Factors," Am. J. Sports Med., **34**(2), pp. 299–311.
[34] Hewett, T. E., Ford, K. R., and Myer, G. D., 2006, "Anterior Cruciate Ligament Injuries in Female Athletes: Part 2, a Meta-Analysis of Neuromuscular Interventions Aimed at Injury Prevention," Am. J. Sports Med., **34**(3), pp. 490–498.
[35] Shin, C. S., Chaudhari, A. M., and Andriacchi, T. P., 2011, "Valgus Plus Internal Rotation Moments Increase Anterior Cruciate Ligament Strain More Than Either Alone," Med. Sci. Sports Exercise, **43**(8), pp. 1484–1491.
[36] McLean, S. G., Lipfert, S. W., and van den Bogert, A. J., 2004, "Effect of Gender and Defensive Opponent on the Biomechanics of Sidestep Cutting," Med. Sci. Sports Exercise, **36**(6), pp. 1008–1016.
[37] Sigward, S. M., and Powers, C. M., 2007, "Loading Characteristics of Females Exhibiting Excessive Valgus Moments During Cutting," Clin. Biomech. (Bristol, Avon), **22**(7), pp. 827–833.
[38] Ajdaroski, M., Tadakala, R., Nichols, L., and Esquivel, A., 2020, "Validation of a Device to Measure Knee Joint Angles for a Dynamic Movement," Sensors (Basel), **20**(6), p. 1747.